



A LETTERS JOURNAL EXPLORING
THE FRONTIERS OF PHYSICS

OFFPRINT

**Transient termination of spiking by noise in
coupled neurons**

B. S. GUTKIN, J. JOST and H. C. TUCKWELL

EPL, 81 (2008) 20005

Please visit the new website
www.epljournal.org

TAKE A LOOK AT THE NEW EPL

Europhysics Letters (EPL) has a new online home at
www.epljournal.org



Take a look for the latest journal news and information on:

- reading the latest articles, free!
- receiving free e-mail alerts
- submitting your work to EPL

www.epljournal.org

Transient termination of spiking by noise in coupled neurons

B. S. GUTKIN¹, J. JOST² and H. C. TUCKWELL²

¹ *Group for Neural Theory, Département des Etudes Cognitives, Ecole Normale Supérieure, Collège de France
5, rue d'Ulm, 75005 Paris, France*

² *Max Planck Institute for Mathematics in the Sciences - Inselstr. 22, 04103 Leipzig, Germany*

received 11 September 2007; accepted in final form 16 November 2007

published online 14 December 2007

PACS 05.40.Ca – Noise

PACS 84.35.+i – Neural networks

PACS 87.16.Ac – Theory and modeling; computer simulation

Abstract – We examine the effects of stochastic input currents on the firing behavior of two excitable neurons, coupled with fast excitatory synapses. In such cells (models), typified by the quadratic integrate and fire model, mutual synaptic coupling can cause sustained firing or oscillatory behavior which is necessarily antiphase. Additive Gaussian white noise can transiently terminate the oscillations by moving the dynamics away from the stable limit cycle. Further application of the noise may return the system to spiking activity. When the noise is sufficiently weak, the durations of the times spent in the oscillating and the resting states are strongly asymmetric. Hence weak noise tends to stop the spiking activity. When the noise is stronger, the periods of cessation of activity tend to be smaller. We numerically investigate an approximate basin of attraction, \mathcal{A} , of the periodic orbit and use Markov process theory to explain the firing behavior in terms of the probability of escape of trajectories from \mathcal{A} .

Copyright © EPLA, 2008

Introduction. – Recent experiments [1] have shown that the spiking patterns of regular spiking and fast spiking neurons in the rat somatosensory cortex exhibit Type-1 and Type-2 behavior, respectively. Such differences were originally found by Hodgkin [2] in his investigations of the responses of squid axon preparations to applied currents. In some cases, the frequency of firing rose smoothly from zero as the current increased whereas in others, a train of spikes with a non-zero minimal frequency suddenly occurred at a particular input current. Cells that responded in the first manner were called Class 1 (which we call Type 1) whereas cells with discontinuous frequency-current curves were called Class 2 (Type 2). Mathematical explanations for the two types are found in the bifurcation which accompanies the transition from rest state to the periodic firing mode. For Type-1 behavior, a resting potential vanishes via a saddle node bifurcation whereas for Type 2 the instability of the rest point is due to an Andronov-Hopf bifurcation; see for example [3].

The stochastic nature of nervous-system activity has been long known (for example, [4]). Methods for modeling and analyzing the stochastic firing activity of single neurons have been well documented [5–10] and the effects of additive noise have been discussed in detail [11]. In uncoupled sensory neurons, noise has been shown to induce synchronized bursting [12]. Here we analyze the

effects of stochastic inputs on the firing behavior of coupled excitable neurons of Type 1, which has not been extensively investigated [13,14]. We identify a novel effect of noise on the firing sustained by recurrent excitatory synapses in a pair of Type-1 neurons: weak noise effectively terminates the firing by taking it out of the basin of attraction of the stable limit cycle. Stronger noise can lead to intermittent oscillatory behavior. Particularly unexpected are simulations that suggest that such an effect is generic and does not depend on the noise model, although our focus is on Gaussian white noise. We explore two analytical approaches to explain the “inhibitory” effect of the noise, one via first-exit time theory and the other using moment differential equations.

The quadratic integrate and fire model and the θ -neuron. – Computational models which include details of the complex anatomy and physiology of cortical neurons are too complicated to analyze mathematically. However, we can take advantage of the generic nature (as the local normal form of a saddle node bifurcation) of a relatively simple neural model that exhibits Type-1 firing behavior. This is the quadratic integrate and fire (QIF) model [15] for which

$$\dot{x} = (x - x_R)^2 + \beta, \quad (1)$$

where x is interpreted as the membrane potential of the neuron, x_R is its resting value and β is the mean input

which is taken to be negative below. (Note that we use the convention that upper (lower) case variables are (non-) random.) Once the value x is so large that the r.h.s. of (1) is positive, it will become infinite in a finite time, and then has to be reset to $-\infty$. The upward excursion and resetting constitute a “spike” in this model. Problems with infinite values can be avoided by applying the transformation $x - x_R = \tan \frac{\theta}{2}$, where θ takes values in $[0, 2\pi]$, *i.e.*, on the unit circle S^1 when we identify 0 and 2π . This yields the θ -neuron model [6,16]

$$\dot{\theta} = 1 - \cos \theta + (1 + \cos \theta)\beta, \quad (2)$$

where $\theta = \pi$ corresponds to a spike of the neuron. Both of these equivalent formulations have been used previously for simulation and analysis of neural dynamics [6,15].

We consider the case of two coupled identical QIF neurons $i = 1, 2$ with noise terms as follows [14]:

$$dX_1 = [(X_1 - x_R)^2 + \beta + g_s X_3]dt + \sigma dW_1, \quad (3)$$

$$dX_2 = [(X_2 - x_R)^2 + \beta + g_s X_4]dt + \sigma dW_2, \quad (4)$$

$$dX_3 = \left[-\frac{X_3}{\tau} + F(X_2) \right] dt, \quad (5)$$

$$dX_4 = \left[-\frac{X_4}{\tau} + F(X_1) \right] dt, \quad (6)$$

where X_1, X_2 are random processes corresponding to the membrane potentials of the neurons while X_3 (X_4) is the synaptic input from neuron 2(1) to neuron 1(2). In these equations, g_s is the coupling strength between the neurons and W_1 and W_2 are independent standard Wiener processes which enter with amplitude σ . The noise terms represent fluctuations in nonspecific inputs to each neuron as well as possibly intrinsic membrane and channel noise. The function F is given by $F(x) = 1 + \tanh(x - x_{th})$, where x_{th} characterizes the threshold effect of synaptic activation [17], so the variables X_3, X_4 take values in the interval $[0, 2]$. Note that here synaptic potentials arrive in neuron 1 (2) when the neuron 2 (1) fires a spike whose amplitude is large enough to activate the synapse.

If we use Itô calculus [18] the corresponding θ -neuron equations then are, with $i = 1, 2$,

$$\begin{aligned} d\Theta_i &= (1 - \cos \Theta_i - (\sigma^2/2) \sin \Theta_i (1 + \cos \Theta_i) \\ &\quad \times [\beta + g_s X_{i+2}])dt + \sigma(1 + \cos \Theta_i)dW_i \\ dX_{i+2} &= -\left\{ \frac{X_{i+2}}{\tau} + F(x_R + \tan(\Theta_{3-i}/2)) \right\} dt, \end{aligned} \quad (7)$$

where $\Theta_i = \pi$ corresponds to a spike of neuron i . Note that at this spike point, the effect of the noise term vanishes. As verified by Gutkin (unpublished), this, together with the strictly positive contribution of the term $1 - \cos \Theta_i$, ensures that the spike point $\Theta_i = \pi$ can only be passed in the direction of increasing values of Θ_i . Therefore, this model is equivalent to the quadratic integrate and fire model with resetting at ∞ . (Note that the extra

contribution to the drift term comes from the Itô calculus. However, the choice of calculus has no bearing on the results obtained.)

For the purpose of this report we choose a negative value for β so that each neuron in isolation will not fire by itself when its potential is near the resting value x_R , but only when perturbed beyond the threshold $x_T = x_R + \sqrt{-\beta}$. As found in [19] for the model given by (3)–(6), without noise, inducing firing in one neuron by perturbing it beyond threshold leads to sustained firing in both neurons when the coupling strength is above the bifurcation value $g_s = g_s^*$. At that value, two heteroclinic orbits between the unstable rest points where one of the neurons is at x_- , the other at x_+ , with x_{\pm} determined by $x_{\pm} = \pm \sqrt{-\beta - g_s \tau (1 + \tanh(x_{\mp} - x_{th}))} + x_R$, turn into a periodic orbit of antiphase oscillations. We then have two stable attractors, the stable rest point where both neurons take the value x_0 determined by the equation $x_0 = -\sqrt{-\beta - g_s \tau (1 + \tanh(x_0 - x_{th}))} + x_R$, and the antiphase oscillator. This behavior is generic insofar as it depends on generic bifurcations. The only nongeneric aspect is the symmetry between the two neurons caused by the fact that they are both modelled with the same parameter values. If the two neurons were equipped with different parameter values, the two heteroclinic orbits between the above saddles would arise at different parameter values, and the basin of attraction of the antiphase orbit would consequently become asymmetric. Note that the dynamics are equivalent for both versions of the model circuit: the QIF and the θ -neuron.

Results and theory. – In the numerical work, the following constants are employed as the standard set throughout: $x_R = 0$, $x_{th} = 10$, $\beta = -1$, $g_s = 100$ and $\tau = 0.25$. In our simulations, we reset the state variables X_1, X_2 to the value $-x_C$ when they reach or exceed the value $x_C = 20$. The initial values of the neural potentials are $X_1(0) = 1.1$, $X_2(0) = 0$ and the initial values of the synaptic variables are $X_3(0) = X_4(0) = 0$. Results such as those in fig. 1 are obtained. The spike trains of the two coupled neurons and their synaptic inputs are shown on the left for no noise. The firing settles down to be regular and the periodic orbit is in part shown in the (x_1, x_2) -plane as the red (on-line) curve in fig. 2.

The effects of weak noise on the spike trains are shown in the right column of fig. 1. In the top portion an example of the trajectory for $\sigma = 0.1$ is shown. Here three spikes arise in neuron 1 and two in neuron 2, but the time between spikes increases and eventually the orbit collapses away from the periodic orbit. In the example (lower right part) for $\sigma = 0.3$ there are no spikes in either neuron. Extensive simulations showed that orbits tended to collapse away from the periodic orbit in the vicinity of the points P_1 and P_2 , as shown in four trials in fig. 2. Here, the red (on-line) curve depicts the stable periodic orbit in the absence of noise and the blue (on-line) curves are trajectories with noise, $\sigma = 0.1$. These random paths

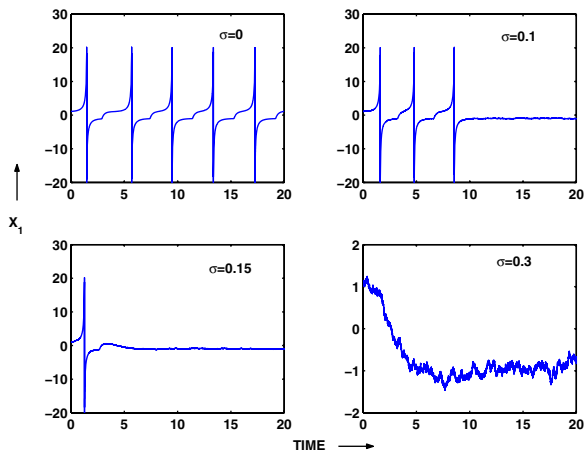


Fig. 1: (Colour on-line) Sample paths for the voltage variable X_1 of neuron 1 obtained from solutions of eqs. (3)–(6) for two coupled QIF model neurons with the standard parameters. In the noise-free case shown in the top left figure, a steady sequence of spikes occurs, with an antiphase sequence in neuron 2. As the noise increases the spiking ceases at earlier times (see fig. 3). Note that these are chosen as representative paths as in the cases with noise there may be zero, one or many spikes.

always start precisely at the same point in R^4 on the periodic orbit —marked as “initial point”. The number of orbits completed is a random variable which we may quantify using T_L , which is the time of occurrence of the last spike in neuron 1. Inspection of histograms of T_L -values, based on 500 trials, for $\sigma = 0.1$ and 0.45 , shows that the spiking stops after approximately an integer multiple of the first spike time. Furthermore, as σ increases, the number of occasions on which no spike was generated increases. This is further illustrated in fig. 3 where the mean of T_L is plotted against σ . Hence it is clear that noise tends to curtail firing. The theoretical basis of these plots is outlined in the next section.

Exit-time and orbit stability. — If a basin of attraction for the periodic orbit can be found, then the probability that the process with noise escapes from this basin gives the probability, in the present context, that spiking will cease. Since the system (3)–(6) is Markovian, we may apply standard first-exit time theory [20]. Let \mathcal{A} be a set in $(S^1)^2 \times [0, 2]^2$ and let y_1, y_2 be the values assumed by Θ_1 and Θ_2 and let y_3, y_4 be the values assumed by the synaptic input variables X_3 and X_4 .

The probability $p(y_1, y_2, y_3, y_4)$ that the process ever escapes from \mathcal{A} is given by

$$\begin{aligned} \mathcal{L}p \equiv & \frac{\sigma^2}{2}(1 + \cos y_1)^2 \frac{\partial^2 p}{\partial y_1^2} + \frac{\sigma^2}{2}(1 + \cos y_2)^2 \frac{\partial^2 p}{\partial y_2^2} \\ & + [1 - \cos y_1 - (\sigma^2/2) \sin y_1 (1 + \cos y_1)(\beta + g_s y_3)] \frac{\partial p}{\partial y_1} \\ & + [1 - \cos y_2 - (\sigma^2/2) \sin y_2 (1 + \cos y_2)(\beta + g_s y_4)] \frac{\partial p}{\partial y_2} \\ & + \left(F \left(x_R + \tan \frac{y_2}{2} \right) - \frac{y_3}{\tau} \right) \frac{\partial p}{\partial y_3} \\ & + \left(F \left(x_R + \tan \frac{y_1}{2} \right) - \frac{y_4}{\tau} \right) \frac{\partial p}{\partial y_4} = 0, \end{aligned} \quad (8)$$

where $(y_1, y_2, y_3, y_4) \in \mathcal{A}$, and with the boundary condition that $p=1$ on the boundary of \mathcal{A} (since the process

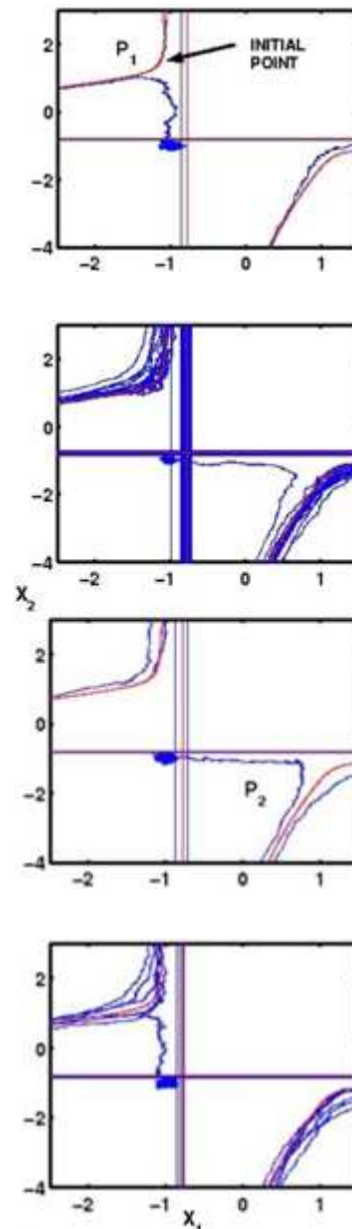


Fig. 2: (Colour on-line) Four examples which illustrate the noise-induced collapse away (blue paths) from the basin of attraction of periodic orbit, denoted by the red curve, in two coupled QIF neurons. The parameters are the standard set, with $\sigma = 0.1$, and the initial point is the same in all cases, being on the periodic orbit as indicated in the top figure. The departure points are located either near P_1 or P_2 . In the top example there is a spike in neuron 2, then a spike in neuron 1 (both clipped) followed by escape from the basin of attraction before a second spike can occur in neuron 2.

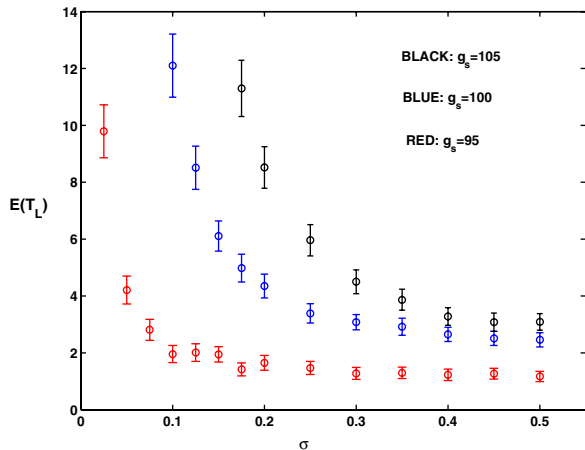


Fig. 3: (Colour on-line) The mean of the time T_L to the last spike in neuron 1 *vs.* the noise amplitude. This quantity measures the exit time from the basin of attraction of the periodic orbit. The 4-dimensional process (X_1, X_2, X_3, X_4) is initially on the periodic orbit. Error bars denote 95% confidence intervals (500 trials).

is continuous). If one also adds an arbitrarily small amount of noise for X_3 and X_4 (or considers those solutions of (8) that arise from the limit of vanishing noise for X_3, X_4), and uses the positivity of the drift term $1 - \cos \theta$ at $\theta = \pi$ where the diffusion coefficient $\frac{\sigma^2}{2}(1 + \cos \theta)^2$ vanishes, the solution of the linear elliptic partial differential equation (8) is unique and $\equiv 1$ so that the process will eventually escape from \mathcal{A} with probability 1. Furthermore, if the expectation of the exit time of the process from \mathcal{A} is denoted by $f(y_1, y_2, y_3, y_4)$ then by a theorem in Markov processes [20] we have

$$\mathcal{L}f(\mathbf{y}) = -p(\mathbf{y}) = -1,$$

with boundary conditions that $f = 0$ on the boundary of \mathcal{A} . We have not attempted to solve this partial differential equation directly, but its solutions correspond closely with the expected value of T_L , the time of the last spike in neuron 1, depicted in fig. 3. In fact, for small noise, the logarithm of the expected exit time from \mathcal{A} , that is, the time at which firing stops, behaves like the inverse of the square of the noise amplitude [21]. When the process escapes from \mathcal{A} , it has to move into the basin of attraction of the stable rest point. With a small probability, noise can eventually also drive the process out of that latter basin, so that some intermittent spiking behavior may result. Near the bifurcation value $g_s = g_s^*$, however, the situation is not symmetric between the two attractors. The width of the basin of attraction of the stable rest point is always positively bounded from below; while just beyond the bifurcation value, the antiphase oscillator basin of attraction is very narrow because it emerges from two heteroclinic orbits linking the fixed points — the rest points and the thresholds, and so, noise can relatively easily drive the dynamics out of it. Numerically, we identified that the

region of easiest escape from that basin is near the points P_1 and P_2 in fig. 2 for the given values of the parameters. This in fact, would be where the basin is the narrowest. It is apparent by examination of the escaping paths and by numerically examining the effects of perturbations away from the periodic orbit that the basin of attraction is narrower to the right of P_1 and to the left of P_2 .

Moment analysis. — Without solving the partial differential equation (8), we may obtain insight into the cessation of spiking activity by using another approach in which the first and second order moments of the variables $X_1(t)$, $X_2(t)$, $X_3(t)$ and $X_4(t)$ are computed. For the set of 4 stochastic differential equations (3)–(6) we may deduce [22], for small noise, a system of 14 coupled ordinary (deterministic) differential equations (ODE) for the first- and second-order moments, being the four means, denoted by $m_i(t)$, $i = 1, \dots, 4$ and the 10 covariances $C_{ij}(t) = \text{Cov}[X_i(t), X_j(t)]$, which includes the 4 variances, $V_i(t)$, $i = 1, \dots, 4$. These equations are given in the appendix. The solutions of these ODEs approximate the moments of the process well when $X_1(t), \dots, X_4(t)$ are approximately normally distributed, as we verified by simulations.

This system of differential equations is easily solved using Runge-Kutta methods. Numerical solutions showed that the variance of X_1 (X_2) suddenly became large in the vicinity of the exit point P_2 (P_1) of fig. 2. Here, P_2 is near the unstable rest point where x_1 takes the value x_+ and x_2 the value x_- . It can be seen from the moment equations that $\frac{dV_1}{dt}$ here is proportional to V_1 with a positive factor m_1 that varies only slowly because $\frac{dm_1}{dt}$ is close to 0 whereas $\frac{dV_2}{dt}$ has the negative coefficient m_2 for V_2 .

Discussion. — We have studied the effect of noise in systems of two coupled neurons of Type 1. The model we have employed is embryonic in the sense that it contains some of the elements of physiological neural networks. The results we have obtained will be a guide to the examination of more complex models to see whether the same phenomena are robust under more general input conditions. Nevertheless, since the quadratic integrate and fire neurons represent the canonical model for Type-1 excitability, our results are generic for that whole class of models. We have found that while coupling can support asynchronous oscillatory activity in excitable neurons, noise can transiently terminate that sustained spiking (near to the bifurcation point where the asynchronous periodic orbit emerges). This circuit is a stochastic analogue of the deterministic case previously studied by Gutkin *et al.* (2001) who showed that transient synchronization can terminate sustained activity. This two-neuron circuit is a minimal circuit model of self-sustained neural activity. Such activity in the prefrontal cortex has been proposed as a neural correlate of working memory [23]. In numerical simulations we have previously noted [14] that the transitions between the two states can be quite

asymmetric, given that the circuit is close to the bifurcation (*i.e.* the synaptic coupling is near the onset of sustained activity). Obviously, for sufficiently weak noise the transition times are long: times for both turning off the sustained activity and turning it on go to infinity as the strength of the noise goes to zero. Strong noise will produce intermitent excursions between the two states, possibly with comparable transition times. However, for a range of noise parameters, depending on the parameters of the circuitry (such as the value of the β and the synaptic time constants), the time to turn off the activity is short while the time to turn it back on (by the noise) is long. In fact previous simulations (see [14]) have lead us to believe that there is an optimal value of the noise to turn off the sustained activity without turning it on for any length of simulation so that the two transition times appear to be on separate time scales, and the noise effectively appears to turn off the sustained firing. We developed a geometrical interpretation, showing that the relative size and the geometry of the basin of attraction for the anti-phase oscillation is the key to this effect. Simulations hint at a different scaling for the mean lifetime of the sustained firing state and the silent state as a function of the noise strength. Hence we would speculate that the tuning for the noise-dependent escape from the basin of attraction of the limit cycle is evocative of stochastic resonance phenomena and may be loosely interpreted as a delay of bifurcation by noise. Such delays have been previously noted for excitable single neurons [24] and more recently for spatially extended systems [25].

Simulations of larger networks with detailed conductance based models of cortical pyramidal neurons coupled with AMPA synapses show a qualitatively similar behavior: weak noise stops the sustained activity. A detailed report on these networks is in preparation. We have also investigated the effects of noise in coupled Type-2 model neurons; these results will also be reported elsewhere.

JJ thanks the Institute des Hautes Etudes Scientifiques in Bures-sur-Yvette (France) for hospitality when this work was performed. BSG was supported by EU MEXT "BIND".

Appendix: Moment equations. – The following system of coupled ordinary differential equations is found [22] for the first- and second-order moments of the stochastic system (3)–(6):

$$\begin{aligned}\frac{dm_1}{dt} &= m_1^2 + \beta + g_s m_3 + V_1, & \frac{dm_2}{dt} &= m_2^2 + \beta + g_s m_4 + V_2, \\ \frac{dm_3}{dt} &= -\frac{m_3}{\tau} + 1 + \tanh(m_2 - x_{th}) - \frac{\sinh(m_2 - x_{th})}{\cosh^3(m_2 - x_{th})} V_2, \\ \frac{dm_4}{dt} &= -\frac{m_4}{\tau} + 1 + \tanh(m_1 - x_{th}) - \frac{\sinh(m_1 - x_{th})}{\cosh^3(m_1 - x_{th})} V_1,\end{aligned}$$

$$\frac{dV_1}{dt} = 4m_1 V_1 + 2g_s C_{13} + \sigma^2, \quad \frac{dV_2}{dt} = 4m_2 V_2 + 2g_s C_{24} + \sigma^2,$$

$$\frac{dV_3}{dt} = \frac{2C_{23}}{\cosh^2(m_2 - x_{th})} - \frac{2V_3}{\tau},$$

$$\frac{dV_4}{dt} = \frac{2C_{14}}{\cosh^2(m_1 - x_{th})} - \frac{2V_4}{\tau},$$

$$\frac{dC_{12}}{dt} = 2(m_1 + m_2)C_{12} + g_s(C_{14} + C_{32}),$$

$$\frac{dC_{13}}{dt} = \left(2m_1 - \frac{1}{\tau}\right) C_{13} + g_s V_3 + \frac{C_{12}}{\cosh^2(m_2 - x_{th})},$$

$$\frac{dC_{14}}{dt} = \left(2m_1 - \frac{1}{\tau}\right) C_{14} + g_s C_{34} + \frac{V_1}{\cosh^2(m_1 - x_{th})},$$

$$\frac{dC_{23}}{dt} = \left(2m_2 - \frac{1}{\tau}\right) C_{23} + g_s C_{34} + \frac{V_2}{\cosh^2(m_2 - x_{th})},$$

$$\frac{dC_{24}}{dt} = \left(2m_2 - \frac{1}{\tau}\right) C_{24} + g_s V_4 + \frac{C_{21}}{\cosh^2(m_1 - x_{th})},$$

$$\frac{dC_{34}}{dt} = \frac{C_{24}}{\cosh^2(m_2 - x_{th})} + \frac{C_{13}}{\cosh^2(m_1 - x_{th})} - \frac{2C_{34}}{\tau},$$

For the validity of the underlying approximation for $\sigma \rightarrow 0$, see [21], p. 56f.

REFERENCES

- [1] TATENO T., HARSCH A. and ROBINSON H. P. C., *J. Neurophysiol.*, **92** (2004) 2283.
- [2] HODGKIN A. L., *J. Physiol.*, **107** (1948) 165.
- [3] RINZEL J. and ERMENTROUT G. B., in *Methods in Neuronal Modeling: From Synapses to Networks*, edited by KOCH C. and SEGEV I. (MIT Press, Boston) 1989.
- [4] FRANK K. and FUORTES M. G., *J. Physiol.*, **130** (1955) 625.
- [5] BURKITT A. N., *Biol. Cybern.*, **95** (2006) 1.
- [6] GUTKIN B. S. and ERMENTROUT G. B., *Neural Comput.*, **10** (1998) 1047.
- [7] HOLDEN A. V., *Models of the Stochastic Activity of Neurons* (Springer, Berlin) 1976.
- [8] LINDNER B., LONGTIN A. and BULSARA A., *Neural Comput.*, **15** (2003) 1761.
- [9] RICCIARDI L. M., *Diffusion Processes and Related Topics in Biology* (Springer, Berlin) 1977.
- [10] TIESINGA P. H. E., JOSÉ J. V. and SEJNOWSKI T. J., *Phys. Rev. E*, **62** (2000) 8413.
- [11] LINDNER B., GARCÍA-OJALVO J., NEIMAN A. and SCHIMANSKY-GEIER L., *Phys. Rep.*, **392** (2004) 321.
- [12] NEIMAN A. B. and RUSSELL D. F., *Phys. Rev. Lett.*, **88** (2002) 138103.
- [13] CASADO J. M. and BALTÁNANAS J. P., *Phys. Rev. E*, **68** (2003) 061917.
- [14] GUTKIN B. S., HELY T. and JOST J., *Neurocomputing*, **58-60** (2004) 753.
- [15] LATHAM P. E., RICHMOND B. J., NELSON B. J. and NIRENBERG P. G., *J. Neurophysiol.*, **83** (2000) 808.

- [16] ERMENTROUT G. B., *Neural Comput.*, **8** (1996) 979.
- [17] TUCKWELL H. C. and MIURA R. M., *Biophys. J.*, **23** (1978) 257.
- [18] ØKSENDAL B., *Stochastic Differential Equations: An Introduction* (Springer, Berlin) 2003.
- [19] GUTKIN B. S. *et al.*, *J. Comput. Neurosci.*, **11** (2002) 121.
- [20] TUCKWELL H. C., *Stochastic Processes in the Neurosciences* (SIAM, Philadelphia) 1989.
- [21] FREIDLIN M. I. and WENTZELL A. D., *Random Perturbations of Dynamical Systems*, 2nd edition (Springer, Berlin) 1998.
- [22] RODRIGUEZ R. and TUCKWELL H. C., *Phys. Rev. E.*, **54** (1996) 5585.
- [23] FUSTER J. M. and ALEXANDER G. E., *Science*, **173** (1971) 652.
- [24] TATENO T. and PAKDAMAN K., *Chaos*, **14** (2004) 511.
- [25] HUTT A., LONGTIN A. and SCHIMANSKY-GEIER L., *Phys. Rev. Lett.*, **98** (2007) 230601.